

Nucleus-nucleus reaction cross sections at high energies: Soft-spheres model

Paul J. Karol

Chemistry Department, Carnegie-Mellon University, Pittsburgh, Pennsylvania 15213

(Received 18 November 1974)

A simple analytical expression is derived for the total nuclear reaction cross section in heavy-ion heavy-ion collisions at high energies based on the semiclassical optical model. Tapered nuclear density distributions are used in conjunction with nucleon-nucleon collision cross sections.

[NUCLEAR REACTIONS Nucleus-nucleus, high-energy; semiclassical calculation of total reaction cross sections, tapered density distributions.]

I. INTRODUCTION

High-energy beams of heavy ions have been available on a limited basis for a number of years. Studies of nuclear reactions induced by 720 MeV α particles at Newport News, 920 MeV α particles at the Berkeley cyclotron, 29 GeV ^{14}N at the Princeton-Penn accelerator, and 29 GeV ^{14}N and 34 GeV ^{16}O at the Berkeley Bevatron have recently been reported.¹⁻¹⁵ The Berkeley BEVELAC¹⁶ anticipates beams of relativistic heavy ions through ^{40}Ar to be accessible in the near future. Rapidly growing interest in these studies comes from the fields of nuclear physics, nuclear chemistry, biomedical sciences, and cosmic ray physics. Besides experimental interest, theoretical enthusiasm has also been aroused.¹⁷⁻²³

A measurement vital to any of these pursuits is the total reaction cross section σ_R for a high-energy heavy ion incident on a complex target nucleus. The hard-sphere model of colliding billiard balls in which $\sigma_R = \pi R_0^2 (A_P^{1/3} + A_T^{1/3})^2$ is simple but inaccurate. The overlap model

$$\sigma_R = \pi R_0^2 (A_P^{1/3} + A_T^{1/3} - b)^2 \quad (1)$$

in its several versions,²⁴⁻²⁶ each essentially a modification of the hard-sphere model, is similarly uncomplicated, but we believe also inaccurate in many circumstances because of the absence of energy dependence and the inability to assign a unique value to the overlap parameter b . Alexander and Yekutieli²⁷ calculated nucleus-nucleus reaction cross sections using available density distribution parameters by numerical integration on a computer. We present here a simple analytical expression for soft-sphere nucleus-nucleus reaction cross sections, one which allows for a tapered density distribution at the nuclear surface. The method,

like that of Alexander and Yekutieli, is based on the semiclassical optical model of Fernbach, Serber, and Taylor²⁸ and uses experimental nucleon-nucleon collision cross sections. The cross section formula should be applicable not only for nucleus-nucleus reactions, but also for any hadron-nucleus system.²⁹ Comparison with available experimental nucleon-nucleus and pion-nucleus cross sections is very satisfactory.

II. MODEL

As with the (point) particle-nucleus calculation of Fernbach, Serber, and Taylor using a uniform target density distribution,²⁸ the total reaction cross section

$$\sigma_R = 2\pi \int_0^\infty [1 - T(r)] r dr \quad (2)$$

reduces to the problem of calculating $T(r)$, the probability that at impact parameter r , the projectile will pass through the target without interacting. The transparency function $T(r)$ is calculated by assuming that interactions result from single nucleon-nucleon collisions in the region of overlap between projectile and target. Implicit in this (impulse) approximation is the restriction of the calculation to high energies. For this reason and to maintain a workable model, Coulomb effects are ignored as are considerations of Fermi motion of nucleons within nuclei, reflection, refraction, the effect of the exclusion principle on the nucleon-nucleon scattering cross section inside nuclei, and the possibility of higher order eclipsing corrections.²²

Calculation of the transparency function is facilitated by referring to Fig. 1. A cylindrical coordinate system is defined in reference to the center

of the target nucleus as the origin 0, the z axis as the beam direction, and r as the impact parameter (of the center of the projectile nucleus $0'$). For fixed (r, z) the probability of interaction per unit path length between z and $z + dz$, called the "thickness function" by Glauber,³⁰ is given by

$$Q(r, z)dz = \bar{\sigma}\rho_T(r, z)\rho_P(r, z)dz, \quad (3)$$

where $\rho_T(r, z)$ and $\rho_P(r, z)$ are the nucleon density distributions of target and projectile, respectively, at point (r, z) . The average nucleon-nucleon collision cross section $\bar{\sigma}$ is given by

$$\begin{aligned} \bar{\sigma}(E) = & \left[\left(\frac{Z_T}{A_T} \right) \left(\frac{Z_P}{A_P} \right) + \left(\frac{N_T}{A_T} \right) \left(\frac{N_P}{A_P} \right) \right] \sigma_{ii}(E) \\ & + \left[\left(\frac{Z_T}{A_T} \right) \left(\frac{N_P}{A_P} \right) + \left(\frac{Z_P}{A_P} \right) \left(\frac{N_T}{A_T} \right) \right] \sigma_{ij}(E), \end{aligned} \quad (4)$$

where $Z_{T(P)}$, $N_{T(P)}$, and $A_{T(P)}$ are, respectively, the proton, neutron, and mass numbers of the target (projectile); σ_{ii} is the proton-proton (neutron-neutron) total cross section; σ_{ij} is the proton-neutron cross section all taken from the experimental nucleon-nucleon values^{31,32} at laboratory kinetic energies $E = E_P/A_P$ where E_P is the projectile lab energy.

The probability that the projectile undergoes no interaction at impact distance r is given by

$$\begin{aligned} T(r) = & \exp \left[- \int_{-\infty}^{\infty} Q(r, z) dz \right] \\ = & \exp \left[- \bar{\sigma} \int_{-\infty}^{\infty} \rho_T(r, z)\rho_P(r, z) dz \right]. \end{aligned} \quad (5)$$

The integral in Eq. (5) is the overlap of target and projectile density distributions for target-projectile separation (r, z) and is obtained from

$$\begin{aligned} \rho_T(r, z)\rho_P(r, z) \\ = & 2\pi \int_{-\infty}^{\infty} d\eta \int_0^{\infty} \rho_T(r, z, b, \eta)\rho_P(r, z, b, \eta)b db, \end{aligned} \quad (6)$$

where the coordinate η corresponds to distance, along the nuclei center-to-center axis ($00'$ in Fig. 1), $\eta = 0$ being the target center. The coordinate b is the projected distance of any point from the η axis. Cylindrical symmetry about the η axis is responsible for the factor of 2π . Nuclear density distributions ρ_T and ρ_P are assumed to be spherically symmetric and, in the (b, η) coordinate system, become $\rho_T(R)$ and $\rho_P(R')$, respectively, where radial variables $R = (\eta^2 + b^2)^{1/2}$ and $R' = \{[(r^2 + z^2)^{1/2} - \eta]^2 + b^2\}^{1/2}$.

For light nuclei, with $A \leq 40$, the density distri-

bution is assumed to be Gaussian

$$\rho(R) = \frac{A}{(a\sqrt{\pi})^3} e^{-(R/a)^2},$$

where a is related to the root mean square radius R_{rms} by

$$a = R_{rms}(1.5)^{-1/2}$$

and experimental R_{rms} values³³ may be employed.

For heavier nuclei ($A > 40$) the form of the nuclear density distribution chosen is one which meets two criteria. First, that it describe the tapered nuclear surface in a manner closely approximating that for the charge distribution determined from electron scattering and muonic atom experiments. Second, the distribution should yield an expression in Eq. (6) which will allow an analytical solution for the reaction cross section σ_R rather than one which mandates a numerical integration. What has been chosen is a "surface-normalized" Gaussian density distribution by which is meant the following: the nuclear density distribution is of the form

$$\rho(R) = \rho(0)e^{-(R/a)^2}, \quad (7)$$

where both $\rho(0)$ and a are treated as free parameters adjusted to reproduce the experimentally determined nuclear surface texture as given, for ex-

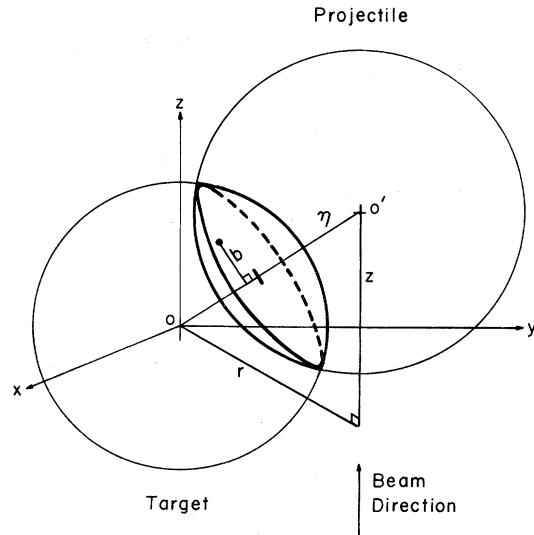


FIG. 1. Coordinate system for the target-projectile overlap integration. The center of the target nucleus is the origin 0; the beam direction defines the z axis; the projected distance of the incident particle center $0'$ from the z axis is the impact parameter r . The points $00'$ define a new η axis about which the target-projectile overlap density is symmetrical. The projected distance of any spatial point onto the η axis defines the b coordinate of that point.

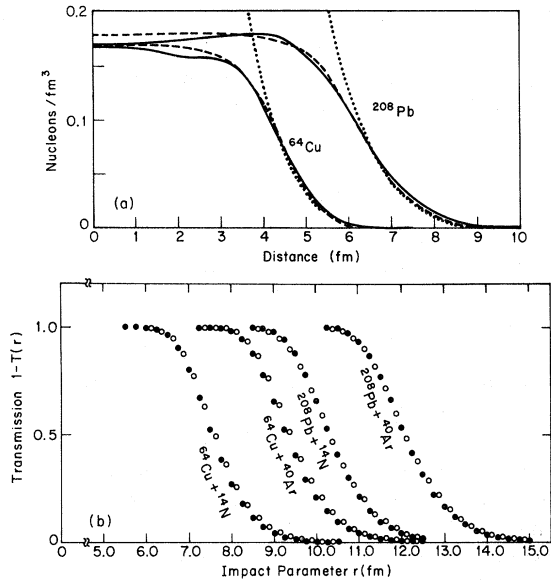


FIG. 2. (a) Nucleon density distributions for ^{64}Cu and ^{208}Pb . The broken curves correspond to Fermi I distributions [Eq. (8)] with $c=4.34$ and $t=2.15$ fm for Cu and $c=6.32$ and $t=2.73$ fm for Pb; the dotted curves correspond to the "surface-normalized" Gaussian distributions [Eq. (7)] which cross the Fermi profiles at the 50% and 10% central density values; the solid curves are the mock "Fermi" density distributions [Eq. (A1)]. Parameters are listed in Table II. (b) Transmission as a function of impact parameter distance for Cu and Pb targets plus N and Ar ions for $\bar{\sigma}=35$ mb. The open circles are evaluated from the surface-normalized Gaussian distributions and the closed circles from the mock "Fermi" distributions shown in (a).

ample, by the usual Fermi I distribution

$$\rho(R) = \rho_0 \{1 + \exp[(r - c)/4.4t]\}^{-1}. \quad (8)$$

The Gaussian density distribution is thus unnormalized, i.e.

$$A \neq 4\pi \int_0^\infty \rho(R) R^2 dR.$$

However, the density distribution in the *nuclear surface* is normalized in the sense that there exists some radial distance, within the half-central-density distance, beyond which the number of nucleons is identical in both the Fermi and Gaussian distributions. Justification for this approach is discussed in extensive detail in the Appendix and may be summarized briefly by recognizing that the transmission, $1 - T(r)$, of the target towards the projectile remains effectively unity at impact

Equation (6) now takes the form

$$\rho_T(r, z)\rho_P(r, z) = 2\pi\rho_T(0)\rho_P(0) \int_{-\infty}^{\infty} d\eta \int_0^\infty \exp\left\{-\left\{\frac{\eta^2 + b^2}{a_T^2} + \frac{[(r^2 + z^2)^{1/2} - \eta]^2 + b^2}{a_P^2}\right\}\right\} b db \quad (12)$$

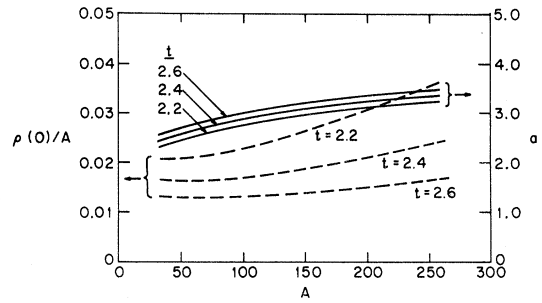


FIG. 3. Graphical illustration of the surface density distribution parameters' dependences on mass number corresponding to $c=1.07A^{1/3}$ and $t=2.2, 2.4,$ and 2.6 fm in Eqs. (9) and (10). Solid curve for a (right scale), broken curve for $\rho(0)/A$ (left scale).

parameters approximately up to the sum of the "radii" of the nuclei regardless of the form of the density distribution chosen for this core-overlap region. Therefore, whether this region is perfectly uniform, hollow, or Gaussian, its contribution to the total reaction cross section is practically geometrical. Beyond this core region the transmission decreases as determined by the texture of the nuclear surface so that the remaining contribution to the total reaction cross section accrues from the skin-overlap region.

Parameters $\rho(0)$ and a for nuclei with $A > 40$ are calculated by requiring $\rho(R)$ at $R=c$ and $R=c+t/2$ in the Gaussian distribution to be identical to the values calculated from the Fermi distribution where c is the half-central-density radius and t is the 90%-10% surface skin thickness parameter usually taken as $1.07 \times A^{1/3}$ and 2.4 fm, respectively. Consequently

$$a^2 = \frac{4ct + t^2}{k} \quad (9)$$

and

$$\rho(0) = \frac{1}{2}\rho_0 \exp(c/a)^2, \quad (10)$$

where

$$\rho_0 = \frac{3A}{4\pi c^3 [1 + (\pi^2 t^2 / 19.36c^2)]} \quad (11)$$

and

$$k = 4(\ln 5) = 6.43775 \dots$$

Example density distributions for ^{64}Cu and ^{208}Pb are illustrated in Fig. 2(a). The dependence of ρ and a on mass number is shown in Fig. 3 for several values of the skin thickness parameter t .

which with the aid of the identities³⁴

$$\int_0^{\infty} x^{2n+1} e^{-b^2 x^2} dx = n! / 2b^{n+1} \quad (13)$$

and

$$\int_{-\infty}^{\infty} e^{-b^2 z^2 + qz} dz = (\pi^{1/2}/b) \exp(q^2/4b^2) \quad (14)$$

becomes

$$\rho_T(r, z) \rho_P(r, z) = \frac{2\pi^{3/2} \bar{\sigma}(E) \rho_T(0) \rho_P(0) a_T^3 a_P^3}{(a_T^2 + a_P^2)^{3/2}} \times \exp[-(r^2 + z^2)/(a_T^2 + a_P^2)] \quad (15)$$

Substitution of the above expression into Eq. (5) followed by integration over the z coordinate yields the transparency function

$$T(r) = \frac{\pi^2 \bar{\sigma}(E) \rho_T(0) \rho_P(0) a_T^3 a_P^3}{(a_T^2 + a_P^2)} \times \exp[-r^2/(a_T^2 + a_P^2)] \quad (16)$$

Finally, the total reaction cross section may be expressed by substituting Eq. (16) into (2) and using the identity

$$\int_0^{\chi} \frac{1 - e^{-u}}{u} du = E_1(\chi) + \ln \chi + \gamma, \quad (17)$$

where

$$\chi = \frac{\pi^2 \bar{\sigma}(E) \rho_T(0) \rho_P(0) a_T^3 a_P^3}{10(a_T^2 + a_P^2)}, \quad (18)$$

$$\gamma = \text{Euler's constant} = 0.5772 \dots$$

for ρ in units of fm^{-3} , a in fm, and σ in mb and the exponential integral³⁵

$$E_1(\chi) = \int_{\chi}^{\infty} \frac{e^{-u}}{u} du$$

$E_1(\chi)$ values are accessibly tabulated³⁵ and usually of negligible magnitude. The final expression for total reaction cross section in mb is

$$\sigma_R = 10\pi(a_T^2 + a_P^2)[E_1(\chi) + \ln \chi + \gamma] \quad (19)$$

in which a_T , a_P , and χ are related to experimental density distribution parameters³³ and nucleon-nucleon cross sections^{31,32} by Eqs. (4), (9), (10), and (18).

The derivative of Eq. (19) provides a quick means of calculating the total reaction cross section $\sigma_R(E)$ at any energy from the 2.1 GeV/nucleon results by application of the approximation

$$\sigma_R(E) \approx \sigma_R(2.1 \text{ GeV}) + [16(A_P^{1/3} + A_T^{1/3}) + 18] \pi \times \ln \frac{\bar{\sigma}(E)}{\bar{\sigma}(2.1 \text{ GeV})} \quad (20)$$

and knowledge of the weighted average particle-nucleon collision cross section in mb at that energy, $\bar{\sigma}(E)$, as given by Eq. (4). Equation (20) is valid for $c = 1.07A^{1/3}$ and $t = 2.4$ fm for projectile and target.

III. RESULTS

Results of the total reaction cross section calculation for 2.1 GeV/nucleon projectiles are illustrated in Fig. 4 and plotted as a function of $(A_P^{1/3} + A_T^{1/3})^2$ for representative targets and projectiles: the figure caption lists all of the parameters which were necessarily employed in the calculation.

Figure 4 demonstrates the nearly linear dependence of σ_R on $(A_P^{1/3} + A_T^{1/3})^2$. Both the hard-sphere model and modified hard-sphere (overlap) model demand linearity. A linear fit to the calculated points in Fig. 4 allows one to determine values of R_0 and b corresponding to Eq. (1). The resulting fitted values of R_0 and b are found to vary both with the target-projectile system and with the free nucleon-nucleon cross section as shown in Fig. 5. Such dependence is not allowed for in the hard-sphere models but is qualitatively reasonable. For light nuclei, b is positive and accounts for some transparency in the mostly skin light nuclei. For heavier nuclei, however, b becomes emphatically negative and in effect accounts for a contribution to the core cross section from the halo of skin nucleons. This is also discernible by noting that b for incident α particles is positive (suggesting transparent encounters) where the free nucleon-

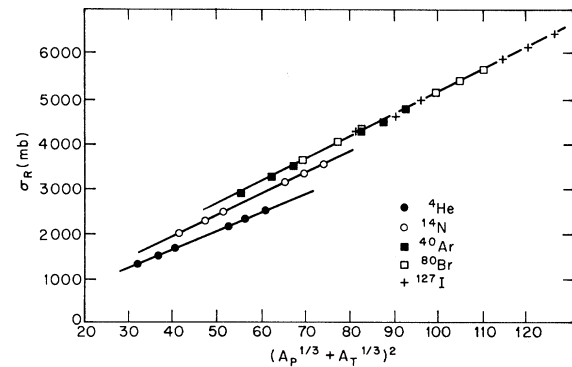


FIG. 4. Nucleus-nucleus reaction cross sections for several projectile systems at 2.1 GeV per nucleon lab energy. Calculated from Eq. (19) using the following parameters: $\sigma_{ii} = 44.9$ mb and $\sigma_{ij} = 43.1$ mb (Ref. 31); $c = 1.07A^{1/3}$ fm and $t = 2.4$ fm for ^{40}Ar , ^{64}Cu , ^{80}Br , ^{89}Y , ^{108}Ag , ^{127}I , ^{181}Ta , ^{208}Pb , and ^{238}U ; $a_P = 1.330$ fm for ^4He and $a_P = 2.074$ fm for ^{14}N . Each projectile system shows a slight curvature but straight lines have been fitted from which hard-sphere overlap parameters R_0 and b are extracted.

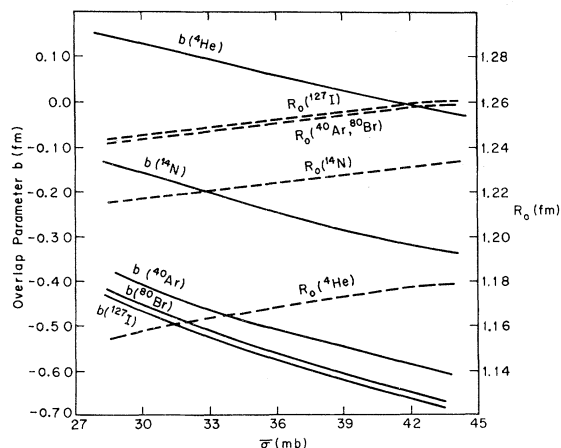


FIG. 5. Dependence of hard-sphere overlap parameters R_0 (right scale) and b (left scale) on the average nucleon-nucleon collision cross section (and therefore projectile kinetic energy) for ${}^4\text{He}$, ${}^{14}\text{N}$, ${}^{40}\text{Ar}$, ${}^{80}\text{Br}$, and ${}^{127}\text{I}$ projectiles.

nucleon cross section $\bar{\sigma}$ is small, but becomes negative as $\bar{\sigma}$ increases in magnitude in order to accommodate the increasing contribution to σ_R from nucleons in the nuclear tail.

Dependence of reaction cross section on projectile energy is well represented by Eq. (20) and exemplified by the excitation function for ${}^{14}\text{N} + {}^{64}\text{Cu}$ in Fig. 6. Dependence of σ_R on the structural parameters c and t is given explicitly if obscurely in the contributing terms of Eq. (19) and is basically dominated by the $\pi(a_T^2 + a_P^2)$ term. Figure 7 shows the variation of σ_R for ${}^{14}\text{N} + {}^{64}\text{Cu}$ with c and t of ${}^{64}\text{Cu}$ extending over reasonable ranges.

Comparison of reaction cross sections predicted by Eq. (19) with experiment is difficult because of the paucity of experimental data. A few such com-

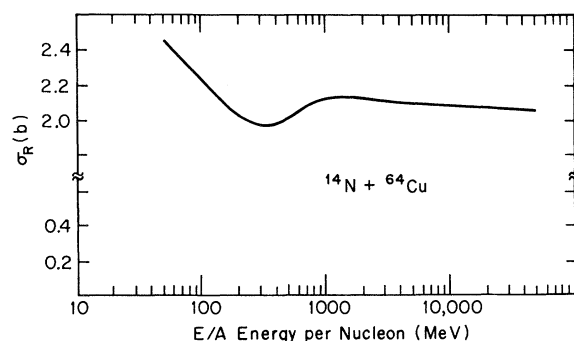


FIG. 6. Excitation function for the total reaction cross section in b of ${}^{14}\text{N}$ incident on ${}^{64}\text{Cu}$ target calculated from Eq. (19). For ${}^{64}\text{Cu}$, $c = 4.28$ fm, $t = 2.4$ fm, $a_T = 2.72$ fm, and $\rho_T(0) = 1.043/\text{fm}^3$. For ${}^{14}\text{N}$, $a_P = 2.074$ fm and $\rho_P(0) = 0.282/\text{fm}^3$. $\bar{\sigma}(E)$'s were obtained from Ref. 32.

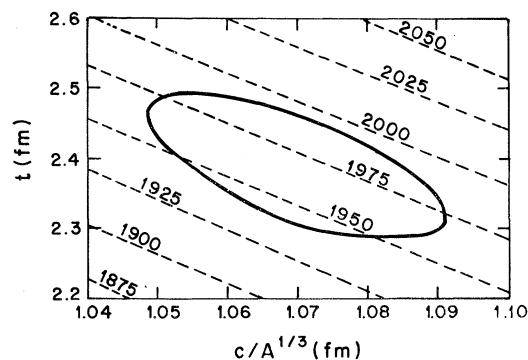


FIG. 7. The ${}^{64}\text{Cu}$ reaction cross section in mb for 2.1 GeV/nucleon ${}^{14}\text{N}$ ions. Dependence of σ_R upon nuclear density distribution radial and skin thickness parameters. The broken curves delineate the constant cross section contours. The heavy closed region encompasses the approximate uncertainties usually associated with experimentally determined values for c , t , and the root mean square radius for ${}^{64}\text{Cu}$.

parisons with high-energy single-particle projectiles³⁶⁻³⁸ and also recent relativistic heavy-ion fragmentation studies of Cheshire *et al.*,¹⁵ are presented in Table I. The agreement is very satisfactory. Preliminary results³⁹ of ${}^{16}\text{O}$ with C, S, Cu, and Pb appear to be systematically low compared to calculation and other data as quoted by Cheshire *et al.*

TABLE I. Particle-nucleus and nucleus-nucleus reaction cross sections in mb. Comparison of experiment with calculated values from Eq. (19).

Projectile	Target	Experiment	Soft Sphere Eq. (19)
20 GeV p	${}^{27}\text{Al}$	472 ^a	497
	${}^{64}\text{Cu}$	850 ^a	847
	${}^{208}\text{Pb}$	1750 ^a	1729
	${}^{238}\text{U}$	1900 ^a	1882
2 GeV π^-	${}^{40}\text{Ca}$	500 ^b	604
	${}^{59}\text{Ni}$	710 ^b	771
	${}^{119}\text{Sn}$	1164 ^b	1188
	${}^{208}\text{Pb}$	1703 ^b	1675
13.3 GeV/c \bar{p}	${}^{64}\text{Cu}$	921 ^c	913
	${}^{208}\text{Pb}$	2026 ^c	1831
13.3 GeV/c K^-	${}^{64}\text{Cu}$	650 ^c	677
	${}^{208}\text{Pb}$	1527 ^c	1505
25 GeV ${}^{12}\text{C}$	CsI	2600 ^d	2740
25 GeV ${}^{12}\text{C}$	W	3000 ^d	3180
34 GeV ${}^{16}\text{O}$	CsI	3000 ^d	2970
34 GeV ${}^{16}\text{O}$	W	3500 ^d	3440

^a Reference 36.

^b Reference 38.

^c Reference 37.

^d Reference 15.

TABLE II. Density distribution parameters.

Parameters	$^{14}\text{N}^a$	$^{40}\text{Ar}^a$	$^{64}\text{Cu}^b$	$^{64}\text{Cu}^a$	$^{208}\text{Pb}^b$	$^{208}\text{Pb}^a$
a	1.77	2.52	1.80	2.51	2.60	3.45
$\rho(0)$	0.602	0.658	0.168	1.62	0.170	2.59
c_0	1	1	1	1	1	1
c_1	0	0	1	0	1	0
c_2	0	0	0.5	0	0.7	0
c_3	0	0	0	0	0	0
c_4	0	0	0.125	0	0.125	0

^a Surface normalized Gaussian density distribution.

^b Mock "Fermi" density distribution, Eq. (A1).

IV. SUMMARY

A relatively simple analytical expression, Eq. (19), is derived which may be used to calculate the total nuclear reaction cross section at high energies for single or composite projectiles on complex nuclei. Known nucleon-nucleon or particle-nucleon free collision cross sections are employed in conjunction with a tapered density distribution which approximates the nuclear tail in both the target and projectile. Calculated results are concordant with the few existing experimental values for composite projectiles.

V. APPENDIX

Equation (19) representing the total reaction cross section between two nuclei with tapered density distributions is justified only if the central "core" regions of the nuclei are completely opaque. Justification of this assumption may be demonstrated by recourse to a comparison of the transparency function for the surface-normalized Gaussian distribution and a more realistic density distribution. For the latter, the form chosen for mathematical convenience is given by

$$\rho(R) = \rho'(0) \sum_{j=0}^N c_j R^{2j} \exp[(R/a)^2] \quad (\text{A1})$$

which, by suitable choice of the c_j 's and a and a limited number of terms N , can reproduce the features exhibited by the Fermi distribution. Example mock "Fermi" distributions for ^{64}Cu and ^{208}Pb are shown in Fig. 2(a). Table II contains the parameters used.

Substitution of the density distribution given by Eq. (A1) into expression (6) can be used to obtain the transparency function $T(r)$ by applying the necessary relationships³⁴

$$\int_{-\infty}^{\infty} x^j e^{-bx^2+2ax} dx = j! e^{a^2/b} \left(\frac{\pi}{b}\right)^{1/2} \left(\frac{a}{b}\right)^j \sum_{k=0}^{j/2} \frac{(b/4a^2)^k}{(j-2k)! k!} \quad (\text{A2})$$

and

$$\int_0^{\infty} x^{2n} e^{-\beta x^2} dx = \frac{(2n-1)!!}{2(2\beta)^n} \left(\frac{\pi}{\beta}\right)^{1/2}. \quad (\text{A3})$$

Equation (5) then provides

$$T(r) = \exp[-q(r)], \quad (\text{A4})$$

where, for a Gaussian projectile density profile

$$q(r) = \frac{\pi^2 \bar{\sigma} \rho'_T(0) \rho'_P(0) a_T^3 a_P^3}{a_T^2 + a_P^2} e^{-r^2/(a_T^2 + a_P^2)} \times \sum_{j=0}^N g_j r^{2j}. \quad (\text{A5})$$

The g_j coefficients are complicated but tractable functions of the representative density distribution parameters c_j , a_T , a_P , and index N . The first term in the sum in Eq. (A5) is a Gaussian term which is identical to Eq. (15) if the parameters are suitably adjusted. Inclusion of higher order terms produces an expression which is not readily amenable to analytical integration. Nevertheless, the functional dependence of $T(r)$ will suffice to validate the approximation under scrutiny. Figure 2(b) shows the transmission $= 1 - T(r)$, or opacity, of ^{64}Cu and ^{208}Pb as a function of impact parameter for high-energy incident ^{14}N and ^{40}Ar ions for the target nuclei density distributions shown in Fig. 2(a) and the parameters in Table II. The projectile nuclei are assumed to have Gaussian density distributions. From the close similarity of the transmissions for Gaussian and flattened target distributions, it seems reasonable to conclude that the location and texture of the nuclear skin determines σ_R . Similar sensitivity to the nuclear surface texture for cross sections of strongly interacting particles has been demonstrated by others.^{40,41}

- ¹P. J. Karol, Phys. Rev. C 10, 150 (1974).
²R. Korteling and E. J. Hyde, Phys. Rev. 136, B425 (1964).
³R. E. Batzel, D. R. Miller, and G. T. Seaborg, Phys. Rev. 84, 671 (1951).
⁴L. B. Church, Phys. Rev. C 6, 1293 (1972).
⁵V. P. Crespo, J. M. Alexander, and E. K. Hyde, Phys. Rev. 131, 1765 (1963).
⁶J. R. Radin, Phys. Rev. C 2, 793 (1970).
⁷J. R. Radin, A. R. Smith, and N. Little, Phys. Rev. C 9, 1718 (1974).
⁸S. Katcoff and J. Hudis, Phys. Rev. Lett. 28, 1066 (1972).
⁹J. B. Cumming, P. E. Haustein, R. W. Stoenner, L. Mausner, and R. A. Naumann, Phys. Rev. C 10, 739 (1974).
¹⁰H. H. Heckman, D. E. Griner, P. J. Lindstrom, and F. S. Bieser, Science 174, 1130 (1971); Phys. Rev. Lett. 28, 926 (1972).
¹¹C. A. Tobias, J. T. Lyman, A. Chatterjee, J. Howard, M. D. Maccabee, M. R. Raju, A. R. Smith, J. M. Sperinde, and G. P. Welch, Science 174, 1131 (1971).
¹²C. A. Tobias, A. Chatterjee, and A. R. Smith, Phys. Lett. 37A, 119 (1971).
¹³J. D. Sullivan, P. B. Price, H. T. Crawford, and M. Whitehead, Phys. Rev. Lett. 30, 136 (1973).
¹⁴L. Skoski, M. Merker, and B. S. P. Chen, Phys. Rev. Lett. 30, 51 (1973).
¹⁵D. L. Cheshire, R. W. Huggett, D. P. Johnson, W. V. Jones, S. P. Roundtree, S. D. Verman, W. K. H. Schmidt, R. J. Kurz, T. Bowen, and E. P. Krider, Phys. Rev. D 10, 25 (1974).
¹⁶H. A. Grunder, W. D. Hartsough, and E. J. Lofgren, Science 174, 1128 (1971).
¹⁷W. L. Wang and R. G. Lipes, Phys. Rev. C 9, 814 (1974).
¹⁸W. Czyz and L. C. Maximon, Ann. Phys. (N.Y.) 52, 59 (1969).
¹⁹O. Kofoed-Hansen, Nuovo Cimento A60, 621 (1969).
²⁰J. Formanek, Nucl. Phys. B12, 441 (1969).
²¹A. Mullensiefen, Nucl. Phys. B28, 368 (1971).
²²G. Fäldt, H. Pilkuhn, and H. G. Schlaile, Ann. Phys. (N.Y.) 82, 326 (1974).
²³A. Y. Abul-Magd, Nucl. Phys. B8, 638 (1968).
²⁴H. L. Bradt and B. Peters, Phys. Rev. 77, 54 (1950).
²⁵R. R. Daniel and N. Durgaprasad, Nuovo Cimento S23, 82 (1962).
²⁶T. F. Cleghorn, P. S. Freier, and C. J. Waddington, Can. J. Phys. 46, S572 (1968).
²⁷G. Alexander and G. Yekutieli, Nuovo Cimento 19, 103 (1961).
²⁸S. Fernbach, R. Serber, and T. B. Taylor, Phys. Rev. 75, 1352 (1949).
²⁹Neutron-nucleus total and reaction cross sections were calculated from a point-projectile plus Gaussian-target model by T. Coor *et al.*, Phys. Rev. 98, 1369 (1955).
³⁰R. J. Glauber, *Lectures on Theoretical Physics* (Interscience, New York, 1959), Vol. I.
³¹D. V. Bugg, D. C. Salter, G. H. Stafford, R. F. George, K. F. Riley, and R. J. Tapper, Phys. Rev. 146, 980 (1966).
³²Particle Data Group, Rev. Mod. Phys. 45, S1 (1973).
³³H. R. Collard, L. R. B. Elton, and R. Hofstadter, in *Nuclear Radii*, edited by H. Schopper (Springer-Verlag, Berlin, 1967), Landolt-Börnstein, New Series, Vol. 2.
³⁴I. S. Gradshteyn and I. M. Ryzhik, *Table of Integrals, Series and Products* (Academic, New York, 1965).
³⁵M. Abramowitz and I. A. Segun, *Handbook of Mathematical Functions* (Dover, New York, 1968).
³⁶G. Bellettini, G. Cocconi, A. N. Diddens, E. Lillethun, G. Matthiae, J. P. Scanlon, and A. M. Wetherell, Nucl. Phys. 79, 609 (1966).
³⁷Yu. P. Gorin, S. P. Denisov, S. V. Donskov, R. N. Krasnokutskii, A. I. Petrukhin, Yu. D. Prokoshkin, and D. A. Stoyanova, Yad. Fiz. 18, 336 (1973) [Sov. J. Nucl. Phys. 18, 173 (1974)].
³⁸B. W. Allardyce, C. J. Batty, D. J. Baugh, E. Friedman, G. Heymann, M. E. Cage, G. J. Pyle, G. T. A. Squier, A. S. Clough, D. F. Jackson, S. Murugesu, and V. Rajaratnam, Nucl. Phys. A209, 1 (1973).
³⁹Comparison of soft-sphere model Eq. (19) with preliminary experimental reaction cross section data of Heckman *et al.* using 34-GeV ¹⁶O projectiles as quoted by Bowman, Swiatecki, and Tsang, in LBL Report No. LBL-2908, 1973 (unpublished).

Target	Experiment	Calculation
¹² C	932	1122
³² S	1310	1710
⁶⁴ Cu	1820	2340
²⁰⁸ Pb	3100	3760

- ⁴⁰D. F. Jackson, Nucl. Phys. A123, 273 (1969).
⁴¹J. P. Auger and R. J. Lombard, Nuovo Cimento 21A, 529 (1974).